Received: 28 May 2020 | Revised: 6 August 2020 | Accepted: 12 August 2020

DOI: 10.1002/er.5942

RESEARCH ARTICLE

INTERNATIONAL JOURNAL OF ENERGY RESEARCH WILEY

Effects of operating parameters and load mode on dynamic cell performance of proton exchange membrane fuel cell

Tien-Fu Yang[1,2] | **Bor-Hung Sheu**[3] | **Mohammad Ghalambaz**[4,5] | **Wei-Mon Yan**[1,2]

[1]Department of Energy and Refrigerating Air-Conditioning Engineering, National Taipei University of Technology, Taipei, Taiwan

[2]Research Center of Energy Conservation for New Generation of Residential, Commercial, and Industrial Sectors, National Taipei University of Technology, Taipei, Taiwan

[3]Department of Mechatronic Engineering, Huafan University, Taipei, Taiwan

[4]Metamaterials for Mechanical, Biomechanical and Multiphysical Applications Research Group, Ton Duc Thang University, Ho Chi Minh City, Vietnam

[5]Faculty of Applied Sciences, Ton Duc Thang University, Ho Chi Minh City, Vietnam

Correspondence
Mohammad Ghalambaz, Ton Duc Thang University, Ho Chi Minh City, Vietnam.
Email: mohammad.ghalambaz@tdtu.edu.vn

Wei-Mon Yan, Department of Energy and Refrigerating Air-Conditioning Engineering, National Taipei University of Technology, Taipei 10608, Taiwan.
Email: wmyan@ntut.edu.tw

Funding information
Ministry of Education (MOE) in Taiwan; Ministry of Science and Technology, Taiwan, Grant/Award Number: 108-2221-E-027-046-MY2

Summary

Utilization of fuel cells as a source of driving power would expose them to dynamic variable loading conditions depending on the driving profile and environmental circumstances. The present research study aims to investigate the dynamic behavior of a single-cell proton exchange membrane fuel cell (PEMFC) subjected to various loading modes and operation parameters. A fuel cell with hydrogen gas as fuel has been assembled as the test module. Three different voltage load modes were designed and applied to the cell. The corresponding current variation of the cell as its dynamic response was measured. The dynamic behavior of the cell was examined for various control parameters such as the cell working temperature, inlet humidification temperature, and stoichiometry. The experimental results indicated that the working temperature of 65°C provided the best fuel-cell performance among the three investigated working temperatures of 45°C, 55°C, and 65°C. At different humidification temperatures, the T_a/T_c = 70°C/60°C humidification condition led to the best fuel cell performance due to the adequate wettability of the membrane. However, the humidification temperature might also have induced a minimal impact on the dynamic response of the fuel cell. Although past studies have indicated that higher stoichiometry achieved better cell performance, the experimental data of this study demonstrated that the cell performance of λ_a/λ_c = 1.5/2.0 was better than λ_a/λ_c = 1.0/1.0 or 3.0/3.0. The influence of the load modes on the performance of the fuel cell was distinguished when the load was high and driving load changed rapidly. Thus, in the present study, the dynamic behavior of a single cell has been investigated and the outcomes can be directly employed for validation of future theoretical models.

KEYWORDS

dynamic load, dynamic response, fuel cell, proton exchange membrane fuel cell, working temperature

1 | INTRODUCTION

As the power source of vehicles, proton exchange membrane fuel cell (PEMFC) benefits from the advantages of low operating temperature, high efficiency, no pollution,

[Correction added on 2 October 2020, after first online publication: the correspondence address of Mohammad Ghalambaz has been corrected in this version.]

and zero-emission.[1,2] These advantages are very promising for future vehicle applications. However, the dynamic nature of loading profiles and variable environmental conditions restrict the commercialization of these fuel cells for vehicles. The design, control, and optimum operation of PEMFCs demand a fundamental understanding of the influence of working parameters on the cell-performance. Moreover, a fuel cell can be subject to various transient load profiles in vehicles and domestic applications. In this situation, understanding the dynamic response of the fuel cell is a crucial factor for the control and optimal design of fuel cells under dynamic loads. There are also very recent patents regarding reducing the impact of dynamic loads on fuel cells.[3] Exergy and energy analysis[4,5] and degradation of PEMFCs under start-stop operating conditions[6] were also reviewed in recent works.[4-6] In a comprehensive review, Chen et al[7] studied the test protocols for the examination of stack fuel cells. Several mathematical models were introduced to investigate the dynamic response of PEMFCs, such as the studies of Lee and Wang,[8] Saadi et al,[9] and Chen et al.[10] Lee and Wang[8] proposed a model to predict the dynamic response of a fuel cell to a sudden load variation. Their results showed that their model was capable of predicting the dynamic and static outlet of the fuel cell. Saadi et al[9] proposed three dynamic models to predict the dynamic response of a fuel cell stack. Their results indicated that the accuracy of dynamic models could be varied about four times in the prediction of the dynamic response of a stack. Chen et al[10] applied several step changes in the inserted loads on a fuel cell. Matlab-Simulink was used for the prediction of the dynamic response of the cell and they stated that their model can be applied for improving the performance and design of fuel cells.

Yun et al[11] and Yang et al[12] considered the dynamic response of fuel cells for the wettability of fuel cells. They proposed numerical models for the analysis of water recovery and humidification of fuel cells. Some of these mathematical models and designs for PEMFCs were reviewed in the study of Blal et al[13] and Hbilate et al,[14] while Zhang and Jiao[15] reviewed water management models of PEMFCs. Mathematical models are beneficial for optimization and understanding the behavior of PEMFCs. However, experimental data are essential to validate the mathematical models and their accuracy. The literature review shows that there are some experimental attempts to identify and analyze the essential parameters affecting the performance of PEMFCs. For example, Yan et al[15] investigated the performance of PEMFC for the variation of the relative humidity, pressure drop, temperatures, and feed gas flow rates. The results displayed that the temperature of the fuel cell and the moisture of cathode inlet gas played a notable role in the performance. Kim et al[16] examined the effect of stoichiometry on the dynamic behavior of a PEMFC. They measured the cell-current response to the rapid change of voltage in fixed flow rates. The results exhibited that the cell response was under the influence of the relative stoichiometry at initial and steady operating conditions. Shen et al[17] measured the internal voltage distribution of a PEMFC corresponding to various magnitudes of air stoichiometry and current densities for steady and transient loading conditions. The outcomes revealed that there was a temporary voltage fluctuation in the fuel cell under the transient loads which was due to air starvation and this could result in the degradation of fuel cell materials.

Santarelli and Torchio[18] studied the effects of operating factors on the performance of a single cell. They used a step current density loading as the test profile and measured the voltage response of the cell and investigated the effects of the operating temperature on the cell. The results disclosed that an increase in the working temperature improved cell performance if both gas streams were sufficiently humidified. When the cell temperature was 80°C, and the gas stream was under low humidification, the cell performance was low, but in high humidification environment, the performance would increase sharply. Wang et al[19] investigated the dynamic response of a PEMFC and the formation and transport of liquid water in the presence of mechanical vibrations. Interestingly, the presence of vibration led to voltage fluctuations. The vibrations also delayed the steady-state performance of the fuel cell. The authors found that a specific vibration amplitude of 4 mm improved the PEMFC performance slightly. Khan et al[20] proposed a semiempirical dynamic model for a PEMFC. The model was tested under specific loads such as ramp load and no-load conditions, and good agreement between the theoretical model and experiments was found. Various aspects of fuel cells, such as their durability,[21] channel design,[22,23] baffle plates design,[24] operation parameters,[25,26] have been addressed in the recent years.

Chen et al[27] analyzed the quality of gas distribution in a PEMFC subject to dynamic loads. They reported that the lack of gas supply due to start-stops and frequent load changes was an essential issue for the life decay of a fuel cell. In a very recent study, Chen et al[2] introduced a starvation index to judge the fuel cell starvation in the process of fuel cell loading. Kim et al[28] explored the effects of excess air ratio, air stoichiometry, and air humidity on the transient response of a PEMFC under step current load changes. The outcomes revealed that voltage drop was elevated by reducing the air stoichiometry and the rise of it intensified voltage undershoots in the fuel cell. He et al[29] reported that the lifetime of fuel cells for vehicle applications was one of the precarious commercialization barriers. The main reason leading to life attenuation

of fuel cells was a regular variation of loading conditions. The dynamic response characteristics and mechanism of fuel cells are not yet evident, and further fundamental studies on the behavior of fuel cells in the process of load change are being demanded.

The literature review demonstrates that the transient and dynamic responses of fuel cells are essential issues that they affect not only the lifetime but also the performance of the fuel cells and moreover, further understanding of the dynamic response behavior of fuel cells is an indispensable task. Hence, the present study objectives to address the dynamic behaviors of a single PEM fuel cell subjected to practical dynamic loads. Furthermore, in the above literature works, a stepwise loading profile has been utilized to test the dynamic response of the fuel cells. However, using a practical driving profile based on the typical road conditions has been overlooked in most of the previous works. Thus, in the current study, three load modes were designed based on practical driving profiles to study the effective response of a fuel cell exposed to practical dynamic loads.

2 | EXPERIMENTATION

2.1 | Experimental setup

The present experiment aims to address the performance of a PEMFC at various fuel cell working temperature, inlet humidification temperature, and stoichiometry, subject to various load scenarios. Hence, a PEMFC-test system (the Fuel Cell and Hydrogen Energy Research Laboratory of the Industrial Technology Research Institute) was utilized. A PEMFC single cell was assembled as the test module. A schematic view of the accessories of the fuel cell and the exploded view of the PEMFC are illustrated in Figure 1A,B. As shown in Figure 1B, the PEMFC single cell consisted of a membrane electrode assembly (MEA) and the gas flow channel on the graphite plate, the gas-tight gasket, the current collector plate, the side plates on both sides, and other supporting parts. An actual image of the PEMFC is shown in Figure 1C,D.

The MEA is the most crucial part of the PEMFC, which directly affects the performance and life of the cell. It contains a polymer electrode membrane and the catalyst layers, the gas diffusion layers on both sides. By diffusion, the reaction gases reach the catalyst layer, where the catalyst increases the reaction rate of the gas by reducing the activation energy of the reaction. The proton exchange membrane was made of a high molecular polymer film. This layer prevents hydrogen gas from penetrating the oxygen and transferring charge. A thin layer of platinum catalyst was plated on both sides of the proton exchange membrane which accounted for about 40% of the fuel cell cost. On the hydrogen side of the proton exchange membrane, hydrogen molecules release positively charged hydrogen ions at the catalyst site and

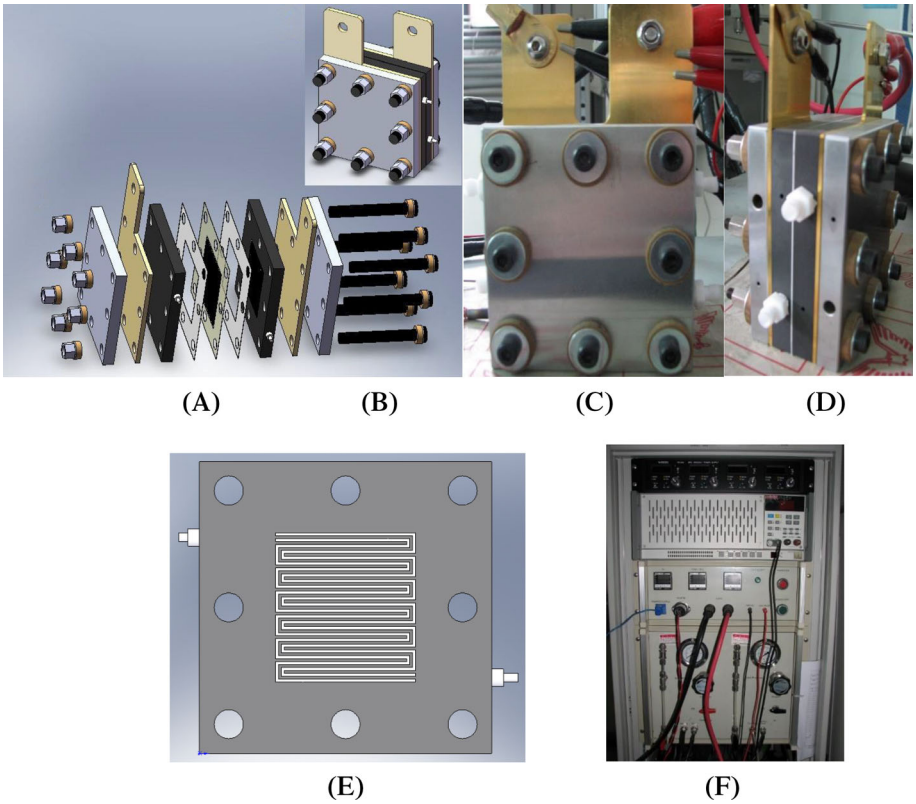

FIGURE 1 Schematic diagram of a PEMFC. A, Combination chart; B, part drawing; C, front view of the physical diagram of the PEMFC; D, side view of the physical diagram of the PEMFC; E, schematic diagram of the flow field of the bipolar plate; F, a photo of the cell test machine [Colour figure can be viewed at wileyonlinelibrary.com]

penetrate the membrane. On the oxygen side of the membrane, hydrogen ions, an electron, and oxygen react chemically in the catalyst layer, producing water.

The upgrading of the membrane performance for reducing the costs and improving its energy consumption is an active area of research. The membrane electrode of the present study was manufactured by GORE-TEX Co., Ltd., model PRIMRA 5621, which was a three-layer structure combining proton exchange membrane and catalyst layer with the reaction area of 5×5 cm^2. The catalyst layer was manufactured by GORE-TEX. The loading of platinum and ruthenium (Ru) alloy on the anode side was 0.45 mg/cm^2, and the platinum alloy on the cathode side was 0.6 mg/cm^2. The total thickness of the catalyst layer and the proton exchange membrane was about 35 μm. The gas diffusion layer (SGL CARBON GROUP; model 10-BC) is made of a porous conductive material, carbon paper, and its primary function is to support the proton exchange membrane and the catalyst layer to enhance its mechanical stability. This layer removed the excess water in the membrane and directed the conduction path of the electrons. The size of the gas diffusion layer was 5×5 cm^2, with a thickness of 400 μm. The material composition of the gas diffusion layer induced hydrophobic behavior.

The bipolar plates (POCO Company; model AXF-5QCF) of the PEMFC were adhered to the gas diffusion layers of the cathode and the anode. The bipolar plates had the functions of an air intake, current collection, and rapid heat dissipation. These bipolar plates were another important factor affecting cell power density and manufacturing cost. Fuel cells relied on bipolar plates to transfer reactive gases and to discharge reaction products. The surface of the bipolar plates was engraved with a number of flow channels for transfer of the reaction gas. The bipolar plate portion of the flow-channel-surface was tightly combined with the gas diffusion layer to form an electron channel. The bipolar plate used in this experiment was made of a high-density carbon plate with an overall area of 10×10 cm^2 and a thickness of 1 cm.

The design of the flow channel is serpentine and aschematic view is shown in Figure 1E. The number of serpentine flow channels was two, and the flow path had a width and depth of 1 mm. The number of turning points was 24, and the flow channel distribution area was 5×5 cm^2. The presence of the turning points increased the shear stress and promoted the gas diffusion into the catalyst; hence, the probability of the electrochemical reaction and the liquid water removal ability inside the gas diffusion layer amended. The gaskets were used to properly tight the multi-layer structure of the PEMFC. The fuel cell was composed of a multi-layer structure, and the materials of each layer were different in type and size, and due to that the joints could not completely seal the PEMFC module. As the fuel cell operated with hydrogen and oxygen, any leakage would be dangerous for the risk of explosion. Hence, a layer of gasket (Teflon 284, model: SG05XL-J; GORE-TEX) was applied between the bipolar plate and MEA on both sides during the assembly of the cell. The elastic and insulating properties of the gasket prevented the leakage and protected the MEA.

The collector plate, with a size of 10×10 cm^2 and a thickness of 0.4 cm, was made of red copper. The surface of the collector was plated with a layer of gold to increase the conductivity and reduce the contact resistance, and prevent the corrosion of the bipolar plate.[30,31] The endplate was located at the outermost part of the cell. Its primary function was to act as clamping support to provide stable support for the cell and its various parts. The two main plates and bolts were used to clamp the main structure of the cell. The endplate of the experiment was made of aluminum alloy 7075 with the size of 10×10 cm^2 and a thickness of 1 cm.

2.2 | Apparatus used

An image of the fuel cell test system is depicted in Figure 1F. The fuel cell test system was assembled by the Green Energy and Environment Research Laboratories of the Industrial Technology Research Institute. The fuel cell test system consisted of five mains parts: a gas supply system, a flow control system, a temperature control system, a humidification system, and an electronic loading system. The overall schematic diagram of the test system is shown in Figure 2. The anode gas was hydrogen, and the cathode had two different inlet gases, oxygen, and air, and the temperature range was from 25°C to 100°C. The maximum power tested by this test system device was 300 W, the maximum current limit was 60 A, and the maximum voltage limit was 60 V. The details of each part have been explained in the following section.

2.2.1 | Gas supply system

The hydrogen, oxygen, air, and nitrogen used in this research experiment were supplied by high-pressure cylinders. In the experiment, the gaseous fuel was firstly decompressed through the cylinder outlet pressure regulating valve of the gas storage cabinet, so that the fuel gas pressure was reduced to about 1.36 atm, and then, a second pressure regulating valve available in the test system was also utilized to adjust the target pressure. The gas was then adjusted by the flow controller, the gas

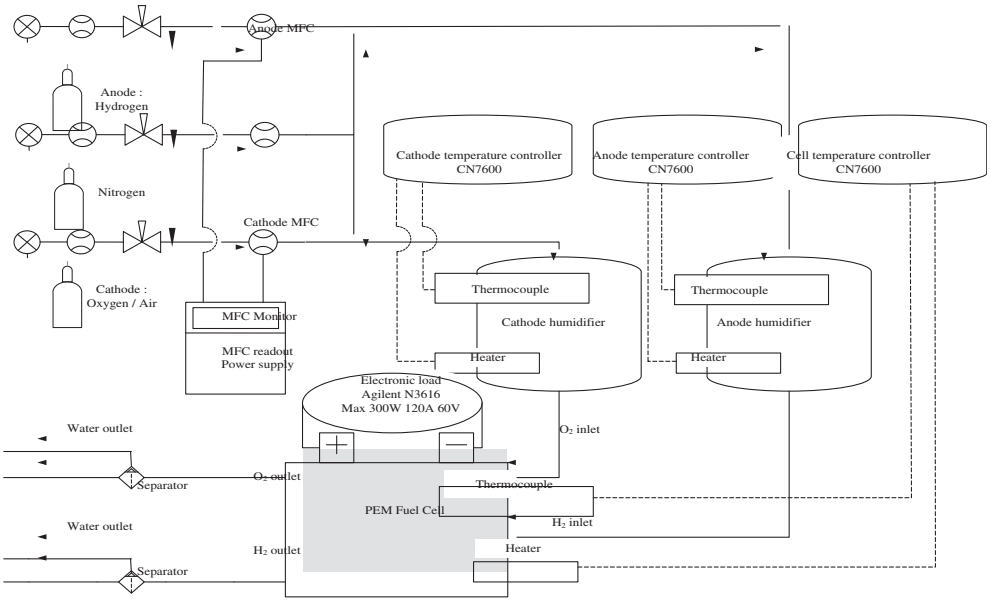

FIGURE 2 Schematic diagram of the fuel cell test system

purification module, and the solenoid valve, and later humidified in the humidification bottle and warmed to a temperature required for the experiment. Finally, the humidified and temperature adjusted gas was introduced into the cathode and anodes of the cell. For nitrogen gas, the primary function of the fuel cell was to remove the residual gas in the pipeline before and after the experiment to ensure the consistency of the cell performance test. The purging of the nitrogen into the pipes safeguarded that the experiment was not affected by the residual gas in the previous experiment. The nitrogen pressure was maintained at around 2 atm during the test. The gas in pipelines was switched using a solenoid value, including the switching of gas such as nitrogen, anode hydrogen, cathode oxygen, or air. In the experiment, hydrogen was flammable and dangerous fuel gas, so the gas cylinders were placed in an outdoor gas storage cabinet for safety reasons.

2.2.2 | Flow control system

Two flow control valves were used with a flow control system consisting of a computer control interface card and a Protec display. The maximum flow rate of hydrogen on the anode side was controlled at 4000 cc/min, and the maximum flow rate of oxygen on the cathode side was controlled at 6000 cc/min. In the experiment, flow control can be divided into two types: one was to control the gas inlet flow rate by stoichiometry and the other to control the minimum flow of the gas inlet. During the test, it was found that if the flow rate was lower than 176 cc/min at the anode or 105 cc/min at the cathode, the fuel cell test system would be very unstable. Hence, in the present study, the anode stoichiometry was adopted as 1, 1.5, and 3, and the cathode stoichiometry was selected as 1, 2, and 3 to be in agreement with the capabilities of the test system, and the influence of different stoichiometry cell performance were investigated.

2.2.3 | Temperature control system

The temperature control system uses a heating rod, a T-type thermocouple, and a CN76000 thermostat to control the internal cell temperature. Three small holes were processed on the side of the endplate. The holes were used as places for inserting the heating rods and thermocouples. The combination of the heating roads and the thermocouple controls the temperature. In this experimental study, the cell temperature was controlled at 45°C, 55°C, and 65°C.

2.2.4 | Humidification system

In the humidification system, the water bottle bubble method was used to humidify the gaseous fuel. The so-called water bottle bubble method was to pass the gas through the humidification bottle in a small bubble manner, and the gas in the humidification bottle was brought to the desired saturation state by humidifying the gas in the bottle. A thermostat was used to adjust the internal water temperature of the humidification bottle, and the water content of the control gas into the fuel cell system was controlled to ensure that the gas passes through the humidification bottle had reached the desired gas humidification temperature. In this experiment, the anode

humidification temperature was controlled at 60°C, 70°C, and 80°C, and the cathode humidification temperature at 50°C, 60°C, and 70°C. The effects of the anode and cathode humidification temperatures on the performance under different humidification temperatures were investigated by changing the humidification temperature of the cell.

2.2.5 | Electronic loading system

The electronic loading system was a model of N3316 produced by Agilent, which was capable of supplying the maximum output power of 600 W, a maximum current of 120A, and a maximum voltage of 60 V. A computer software (Giant An Technology Workroom) was used to control the voltage load, and the corresponding current, current density, and power value were measured.

2.3 | Experimental methodology

In order to perform the experiment, the following strategies were followed. The experiment was commenced by connecting the cable and voltage measuring line of the electronic load to the cathode and anode according to their polarity (+ cathode, − anode). The residual gas and water generated by the chemical reaction were discharged into the liquid-gas separator by a pipeline. The water level of the humidifying bottle was checked. The water level of the humidifying bottle can be adjusted by using deionized water, which was packed in a steel cylinder and pressurized with nitrogen. The high-pressure gas cylinder line-switch connecting oxygen (or air), nitrogen, and hydrogen were activated, and then the tube pressure regulating valve was adjusted to about 1.36 atm. The pipeline valves were opened to introduce the gas into the test system. In this experiment, the reaction area of the MEA was 25 cm^2. The minimum flow rate was set at 176 and 105 cc/min for the anode and cathode, respectively. The stoichiometric numbers of the anode and cathode were 1.5 and 2, respectively.

Nitrogen gas was introduced in the pipelines of the test system and fuel cell to remove the impurities before and after the test for 15 minutes. The nitrogen removed residual hydrogen, oxygen, and water from the fuel cell. After 15 minutes, the nitrogen feed was turned off, and the test system was activated by adjusting the experiment temperatures. The anode and cathode gas switches were activated to feed hydrogen, oxygen (or air) into the fuel cell and initiation of reactions. The software would adjust the operating voltage based on the defined loading profiles. When the temperature of the cathode and anode humidification bottles and the temperature reached the test target values, the fuel cell performance curves were measured. In this experiment, the fuel cell performance test was performed in a constant voltage mode, and the initial voltages are measured from 0.95 V. This procedure was repeated for all of the different test conditions. Since residual hydrogen, oxygen (or air), and water remained inside the fuel cell after each test, the fuel cell was repurified by disconcerting the reaction gases and introducing nitrogen into the fuel cell for 15 minutes.

3 | EXPERIMENTAL LOADING MODES

This study predominantly is concerned about the effects and changes of cell performance on the vehicle travel under different load propulsion. In order to better meet the changes between the travels, two different load series were adopted, and a series of energy consumption load modes was used. The tests were performed indoors and they had stagnation time at each stage. The other series was the road driving load mode and a road map was used as a reference to design the load that encountered the dynamic fluctuation of the travel which has been explained as follows:

The vehicle energy consumption loading mode mainly adopted the test type specified by each country for the new car factory. There were three different load modes and to compare the differences, the three test load modes were designed with a similar period of the 2460 seconds. The first load type was modeled after the Economic Commission for Europe (ECE) vehicle model and is depicted in Figure 3. The test procedure for load mode 1 was divided into three steps. The first part was an

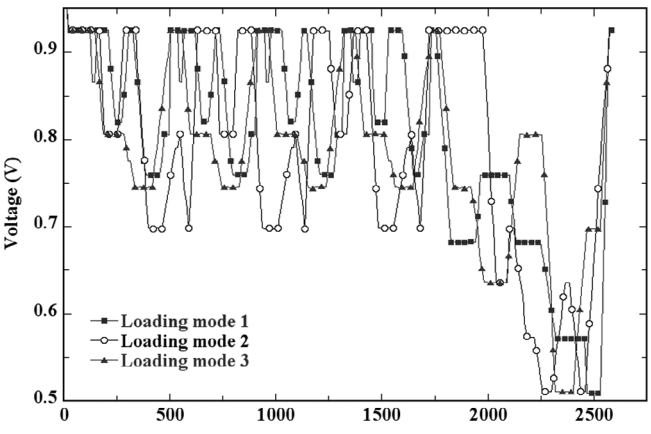

FIGURE 3 The profile of the load modes (x-axis is the time in seconds): Load model 1 is the ECE model, Load mode 2 is the ECRL Japanese model, and Load mode 3 is the self-made model

idle load of 0.95 V for 80 seconds. The second part was for 4 cycles of a traditional urban model, in which each cycle was 390 seconds with a maximum load of 0.759 V and a total time of 1560 seconds. The third part was for 800 seconds of the suburban model with a maximum load of 0.508 V. Hence, the entire test time of load mode 1 was 2460 seconds.

The second load type, load mode 2, was modeled after the Japanese model of 10/15 mode based on Energy Consumption Rationalization Law (ECRL), as revealed in Figure 3. The test procedure was divided into three steps. The first part was the idle load of 0.95 V. The second part consisted of three cycles of 10 Mode-line Japanese model. Each cycle is 520 seconds, with the maximum load of 0.696 V. The total of the three cycles was 1560 seconds. The third part was the model of the 15 Mode-line with a test time of 810 seconds and a maximum load of 0.505 V. As a result, the total measurement time of load mode 2 was the 2460 seconds.

The final load type, Load Mode 3, was the modified self-made vehicle model, as shown in Figure 3. The test procedure was divided into three steps. The first part was 0.95 V idle speed for 80 seconds. The second part was made of three cycles of the medium and low-speed model with a cycle time of 390 seconds and a maximum load of 0.743 V. The total time of these three cycles was 1560 seconds. The third part of load mode 3 was the high-speed line mode with a sharp deceleration part. The test time was 800 seconds, and the maximum load was 0.51 V, so the total measurement time of load mode 3 was 2460 seconds.

4 | RESULTS AND DISCUSSIONS

The performance of the fuel cell itself was susceptible to many parameters, such as mass transfer loss, hydrothermal management, and ohmic resistance. These operating conditions possessed varied degrees of influence on the interior of the PEMFC. In terms of transportation, the fuel cell load had a rapid change and instability due to changes in the external environment. Therefore, this study was aimed to investigate the effects of different operating parameters such as the fuel cell working, inlet humidification temperature, stoichiometry, and low-temperature environment on the dynamic performance response of the PEMFC. The load mode 1 was considered as the reference load mode, and the impact of various parameters in this load mode have been investigated. Thus, for the sake of brevity, the term of load mode 1 was repeated in the text. For PEMFC, many operating parameters directly affected their performance, while the more common operating parameters were fuel cell temperature, inlet humidification temperature, and stoichiometry. An appropriate fuel cell temperature could accelerate the electrochemical reaction rate in the catalyst layer by improving the participation of the gas. It would also increase the transmission speed of ions in the proton exchange membrane, which promoted the performance. A proper humidification temperature could provide sufficient humidification of the membrane. Increasing the conductivity of the membrane can further reduce the transmission impedance inside the fuel cell. Sufficient gas flow could make the fuel supply inside the fuel cell intact, and the phenomenon of mass transfer loss was less obvious which could also increase the water removal capability inside the flow channel. Occasionally, the operating condition of the vehicle was in a relatively low-temperature environment, such as mountains and snow. Hence, the reaction performance of the cell in a low-temperature environment was also essential. Therefore, in this study, the fuel cell temperature, fuel inlet humidification temperature, stoichiometric, and low-temperature effects were considered as parameters to explore the dynamic response of the performance under different load types.

4.1 | Influence of the fuel cell temperature

The fuel cell temperature would directly affect the ion conductivity and current density of the membrane. Excessive temperature would cause the water inside the cell to be excessively removed, which might cause membrane dryness. However, a too low fuel cell temperature will causes water flooding.[32] In contrast, an adequate temperature reduced the need for activation energy in the catalyst layer and improved the reaction rate. Hence, fuel cell operating temperature was an essential parameter, and was selected to investigate the dynamic effect of temperature on the current density of the fuel cell. In this experiment, three temperatures of 45°C, 55°C, and 65°C were examined and the relationship between the output voltage and the current density is measured.

Figure 4A illustrates the influence of the operating temperature on the static performance of the cell in the form of the *i-V* curves. The stoichiometric number was $\lambda_a/\lambda_c = 1.5/2.0$, with the fuel inlet humidification temperature $T_a/T_c = 70°C/60°C$. The results are plotted for the three working temperatures of 65°C, 55°C, and 45°C. As seen, the current density was 0.95, 0.8, and 0.7 A/cm^2 for the working temperatures of 65°C, 55°C, and 45°C, respectively, when the current-voltage was 0.7 V. Figure 4A demonstrates the improvement of fuel cell performance by the growth of the working temperature. This

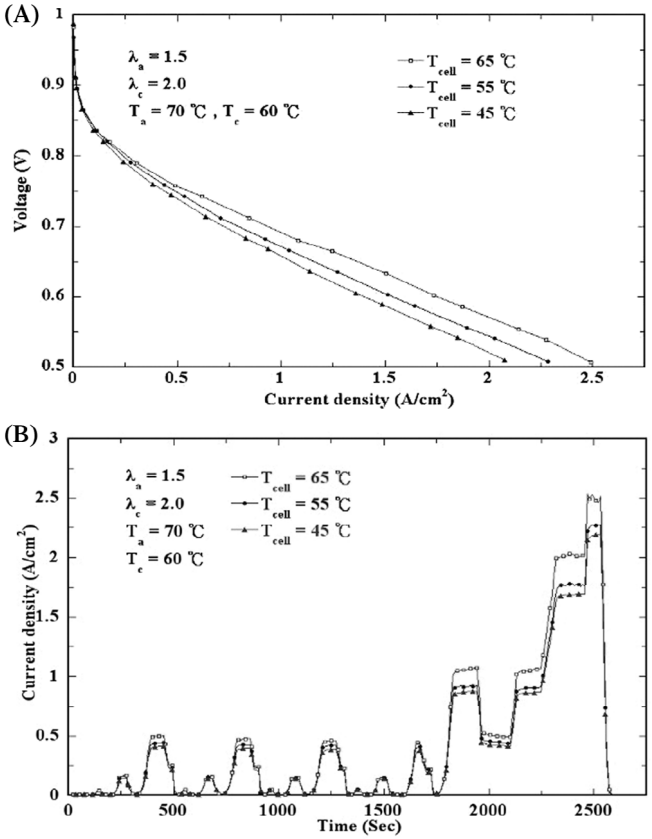

FIGURE 4 Effect of the working temperature on the fuel cell performance. A, Steady-state response and, B, dynamic response

increase was attributed to the promotion of the reaction efficiency of the catalyst by boosting the catalytic effect on the fuel gas, and consequently, generating a high power output. When the working temperature was 65°C, the fuel cell performance was at its best, which indicated that the limit of the operating temperature was not yet achieved. The performance at temperature 45°C was the most minimum, which exhibited that the temperature was too low to effectively internalize the cell moisture removal under inlet humidification conditions. This caused water to accumulate in the fuel cell after the reaction, leading to water flooding of the electrode.[33] Moreover, too low temperature might increase the activation energy required by the catalyst, resulting in a slower electrochemical reaction and a lower current density.

The effects of different working temperatures on the dynamic response of the cell are depicted in Figure 4B. The results have been reported for the three selected temperatures, that is, 65°C, 55°C, and 45°C, when $\lambda_a/\lambda_c = 1.5/2.0$, and the fuel inlet humidification temperature $T_a/T_c = 70°C/60°C$. The experimental results confirmed that the performance difference between the three cell temperatures was not notable in the urban driving cycle, but the performance might increase with the increase of temperature, and the three load modes would quickly reach the specified voltage. At 65°C, it was observed that the performance was slowly rising, but other temperatures did not possess this phenomenon. When the working temperature was high, the reaction was too fast, and more water was needed to wet the membrane. It was expected that the repeated load mode provided similar current density, but from the four load patterns, it was obvious that as the number of tests increases, the performance obtained was gradually reduced for the same load operation mode. Although there was an interval between the repeated loads, the time was too short; so that the gas was not effectively replenished thus resulting in mass transfer loss. In the suburban driving part, which was a high load mode, it can be seen that the performance was increased with the increase of the temperature. However, the performance did not improve at an insufficient temperature of 55°C. There was a slow rising of performance in the cell current density, which was more obvious at 65°C. The raise in performance showed an oscillating phenomenon behavior. The high temperature of the cell contributed to internal water removal. In contrast, the low temperature of 45°C indicated that there was no performance rise at this temperature. The too low-temperature triggered excess internal moisture. At the highest load, it was observed that there was a shock at 65°C, which was caused by the high temperature of the cell. The heat generated by the cell was high and removed a notable amount of the internal moisture, which led to insufficient internal humidification, and thereby a performance fluctuation was observed.

4.2 | Effects of fuel inlet humidification temperature

A higher fuel inlet humidification temperature contains a higher amount of water, which can be used to wet the membrane and reduce the transmission impedance and thereby promoting fuel cell performance. The increase of the humidification temperature improves the hydrogen-oxygen reaction at the catalyst and overcome the performance degradation caused by insufficient gas concentration. However, the excessive inlet humidification temperature is likely to cause internal water flooding.[32,33] When the fuel cell temperature is too high, the membrane inside the fuel cell loses its moisture, and the ion transportability reduces. The dryness of the membrane results in the elevation of impedance and the ohmic losses. Therefore, the fuel inlet humidification temperature is a significant parameter. In this experiment, the inlet humidification temperature was set to three

combinations of T_a/T_c = 60°C/50°C, 70°C/60°C, and 80°C/70°C in order to investigate the change of inlet humidification temperature on the current density and power output of the fuel cell.

The effect of fuel inlet humidification temperature on the steady-state performance of the cell is plotted in Figure 5A. Figure 5B shows the dynamic response to a dynamic load. The results were plotted for a fixed working temperature of 65°C, the stoichiometric number λa/λc = 1.5/2.0, and three different humidification conditions. The most inferior performance was for the humidification temperature of 60°C for the anode and 50°C for the cathode. This might be because of the fact that when the humidification temperature was too low, the gas contained less water, which intensified the membrane dryness inside the fuel cell. As a result, the electrochemical reaction rate deteriorated and the amount of ion transported in the proton exchange membrane declined. At the humidification temperature of T_a/T_c = 70°C/60°C, the fuel cell performance was similar to the case of T_a/T_c = 80°C/70°C. Hence, it was concluded that the fuel cell reached a saturation state of humidification temperature at this stage. Further increase of humidification temperature was not suitable as the produced water after the reaction may cause the flooding problem and decrease the fuel cell performance.

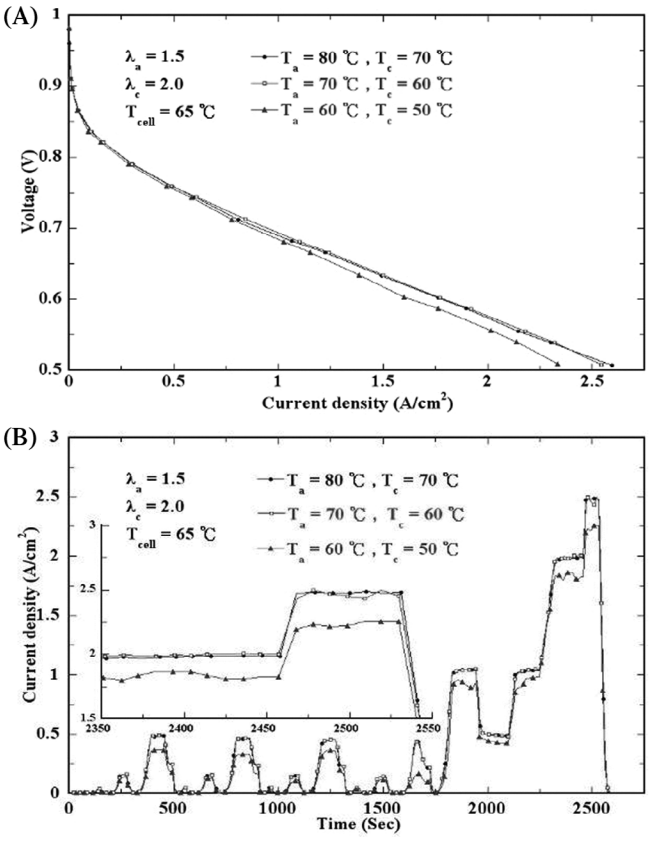

FIGURE 5 Effect of inlet humidification temperature on the fuel cell performance. A, Steady-state response and, B, dynamic response

Figure 5B explores the dynamic response for variable loads. It was found that the increase of the humidification temperature could increase the internal moisture of the fuel cell and reduce the impedance, and thereby effectively improving the fuel cell performance. The steady-state behavior of the cell illustrated that the humidification temperature Ta/Tc = 70°C/60°C can be considered as the saturation temperature. In the urban part of the dynamic load, as depicted in Figure 5B, it can be seen that the performance of the cell was degraded every time the load cycle occurs. In the case of continuous cycle operation, the operation of the fuel cell accelerated the water removal, and the water consumption of the membrane improved. In the suburbs part of the dynamic load, the increase of humidification temperature amplified the performance, particularly in the period of 2350 and 2550 seconds. At a higher load, the heat generation of the cell, and consequently, the water consumption elevated. So, the performance of the fuel cell, which suffered the lack of humidification, showed an oscillating behavior. At a low humidification temperature, the phenomenon of environmental shock occurred because the condition was close to the limit value of the cell dryness. In terms of the transient performance of the cell, it was observed that the low humidification condition slowly extended a stable performance, while the high humidification quickly and smoothly compensated with the load profile. This was because an inlet with a high humidification temperature contained a sufficient amount of water, and even if the load changed to a high level, it supplied enough water. In contrast, other humidification temperatures could not provide the required amount of water, and hence, the fuel cell required a long time to reach a stable performance.

4.3 | Effect of stoichiometry

Gas flow would directly affect the operation of the cell and it is one of the most critical conditions for fuel cell behavior. Increasing the inlet flow rate will improve the concentration of fuel, and consequently, the diffusion rate of the gas inside the fuel cell grows. In return, an increase in fuel cell performance would be expected, but the fuel cell was also limited in flow rate. If the performance exceeded this limit value, the performance will not increase significantly, and there may be a counter effect. The general flow can be provided as a fixed flow or fixed stoichiometry and in this study, the fixed stoichiometry approach was used. This was because the fixed

stoichiometry can change the flow with the load so that the gas flow will decrease when the load was low. This approach was noticed to be economical. Three stoichiometries of λ_a/λ_c = 1.0/1.0, 1.5/2.0, and 3.0/3.0 were examined to investigate the effects of stoichiometry and fuel cell performance.

Figure 6A depicts the effect of stoichiometry on the steady-state performance of the fuel cell. The fuel cell working temperature was fixed at 65°C, and the fuel inlet humidification temperature T_a/T_c = 70°C/60°C was used to supply the fuel. The current density of the cell was affected by the steady-state performance of the cell. From Figure 6A, it can be found that the worst performance was the stoichiometric number λ_a/λ_c = 1.0 / 1.0. A low stoichiometry resulted in the consumption of the fuel in the early length of the cell channel and reduction of mass transfer. In contrast, a high value of stoichiometry would not be able to eliminate internal water effectively. When the stoichiometric number λ_a/λ_c = 3.0 /3.0, the fuel cell performance was worse than the stoichiometric number λ_a/λ_c = 1.5 / 2.0, particularly at low loading voltages. This was because too high gas flow increased the velocity of the gas and reduced the diffusion of the gas into the catalyst layer to participate in the reaction. Moreover, if the excessive flow rate exceeded the reaction limit of the catalyst, there was no apparent effect on performance improvement except fuel wastage. So choosing the right amount of stoichiometry can help improve the fuel cell performance.

Figure 6B displays the effect of stoichiometry on the dynamic response of fuel cell performance. The outcomes revealed that the stoichiometric number λ_a/λ_c = 1.5/2.0 was the best, and the stoichiometric number λ_a/λ_c = 1.0/1.0 caused reduced cell performance. In the urban part of the dynamic load, the difference between the tested stoichiometric ratios was not significant because the test strokes were all at low loads. The outcomes revealed that the stoichiometric number λa/λc = 1.0/1.0 was not sufficient for the fuel cell reaction in the suburban test part as a high load test required more fuel. If the stoichiometry was not enough, the amount of the transferred mass transfer would have been insufficient for catalyst reaction. According to the highest load in the figure, the performance of the stoichiometric number λ_a/λ_c = 1.5/2.0 was considered as sufficient. In this case, when the load was switched to high load, there was an instantaneous performance improvement phenomenon, which meant that there may be residual gas in the flow channel that has not reacted yet, so the performance was improved when the load was increased. When the load was at a high magnitude, the performance oscillated around the equivalent high stoichiometry test results.

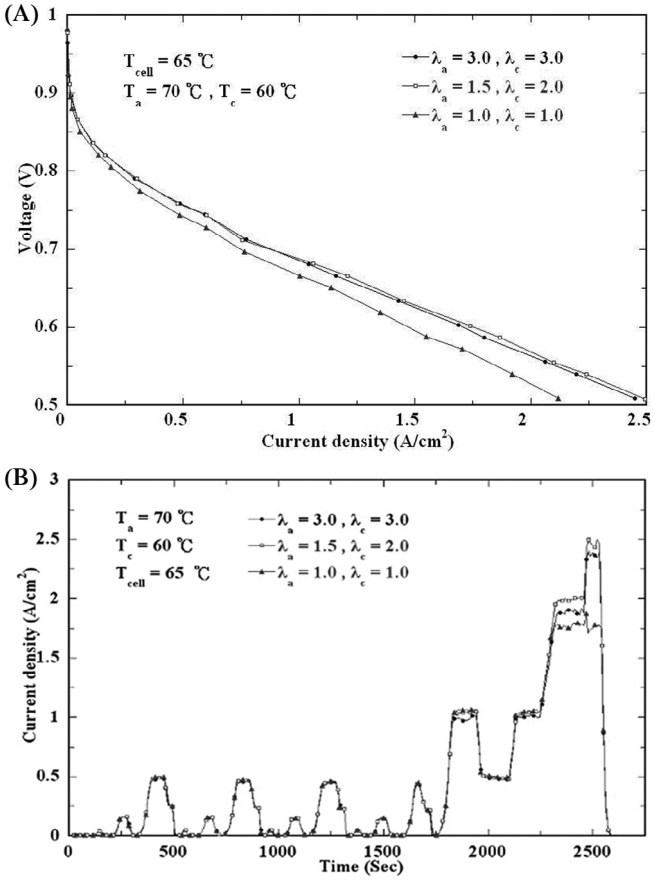

FIGURE 6 Effect stoichiometry on the fuel cell performance. A, Steady-state response and, B, dynamic response

4.4 | Effect of vehicle energy consumption mode on the dynamic performance

Figure 7 shows the impact of different energy consumption modes (load modes) on the fuel cell dynamic performance. The profiles of the load modes were in the form of dictated voltage profiles as described in Figure 3. The fuel cell dynamic responses, corresponding to the load modes of Figure 3, are plotted in Figure 7. Figure 7A,B shows the results for the optimized working temperature of 65°C and a low working temperature of 45°C, respectively. As shown in Figure 7A, the performance of load mode 1 will gradually decreased with the number of repetitions in the first half of the repeat cycle in the urban part of the test. This was due to the frequent load formation, so due to lack of supply gasses, the performance decreased. There were only three cycles in load mode 2 and although the load setting was high, it was one cycle less than the other two load modes. Hence, in the case of load mode 2, the performance-decline was not apparent. In this case, the performance quickly reached

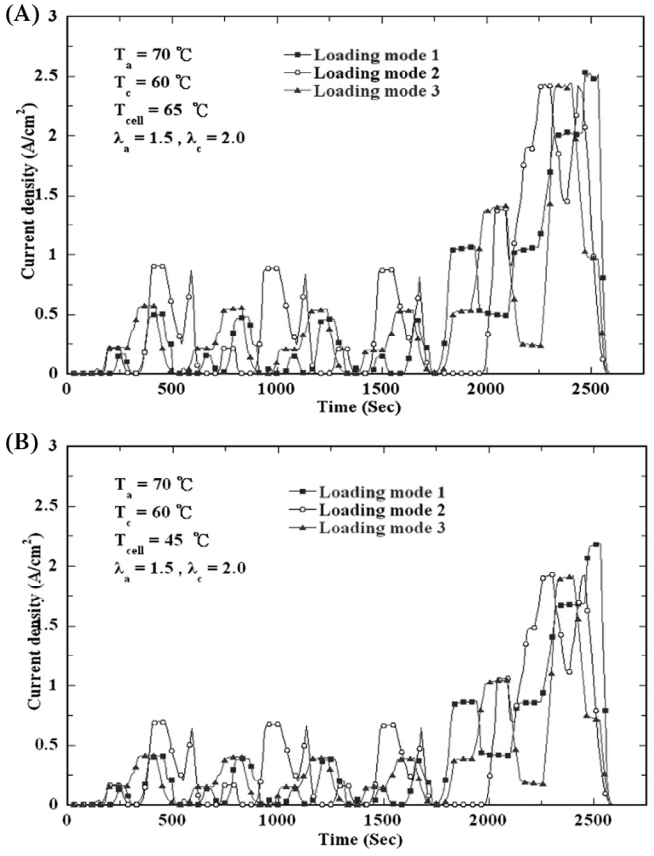

FIGURE 7 Dynamic response of fuel cell subject to various load modes for, A, optimized working temperature of 65°C and, B, a low working temperature of 45°C

equilibrium, and the first cycle showed signs of increase. If the time was too long, there would have been unused residues fuel inside the cell so that the performance may increase. In load mode 3, it was noticed that although the same cycles as the load mode 1 required to be repeated four times as there was no performance reduction in load mode 3. This was because that the difference between the maximum and minimum values of the applied voltages in load mode 3 were smaller than those of load mode 1 during the mentioned cycles, and hence, the cell performance was more unwavering. In the second half of the higher load setting, the cell performance changed rapidly with the load setting, and performance fluctuations occurred at the highest load. This was because the operating conditions were optimized for the fuel cell at 65°C. So, at the highest load, the performance reached its limit and started to oscillate. In terms of average power consumed, the total power consumption was divided by the total time. The average power consumed by load mode 1 was 0.72 W; the average power consumed by load mode 2 was 0.83 W, and the average power consumed by load mode 3 was 0.74 W; hence, more energy was consumed in load mode 2.

Figure 7B monitors the impact of the load profiles at the cold working temperature of the fuel cell. This figure revealed that the performance of the first half cycle changed rapidly. There was still a decline in the performance of the repeated load at the later stage. In this situation, the performance dropped from 0.5A/cm^2 to 0.4 A/cm^2 (load mode 1). A drop from 0.9 to 0.7 A/cm^2 was notified in load mode 2, while a decrease from 0.6 to 0.35 A/cm^2 was observed in the load mode 3, which was the most obvious performance degradation in the three load modes. This notable performance degradation indicated that load mode 3 was not suitable for low-temperature environments. There was a performance enhancement in the steady parts of the high load profiles. This was because the generated reaction heat in the cell improved the electrochemical reaction and performance. At 65°C, the highest performance of the three modes reached 2.5 A/cm^2. While the current density barely reached 2A/cm^2 at a low working temperature of 45°C, only the load mode 1 extended to a value larger than 2A/cm^2 at the highest load. In the cold working status, there was no oscillation, and the performance slowly enhanced. In terms of average power consumption, the average power consumptions in load mode 1, load mode 2, and load mode 3 were 0.62, 0.65, and 0.56 W, respectively. The consumable energy of load mode 2 was the maximum. Compared with the performance of 65°C, the power change in load mode 1 was the minimal, which indicated that the load mode was less affected by temperature changes.

Figure 8 shows the effect of load modes on the dynamic response of the cell when the working temperature was 65°C, and the inlet humidification temperature was T_a/T_c = 70°C/60°C. Figure 8A,B is plotted for the stoichiometric numbers λ_a/λ_c = 1.0/1.0 andλ_a/λ_c = 3.0/3.0, respectively. As shown in Figure 8A, in the low-load cycle part of the figure, the response quickly reached stability without delay, and when compared with a higher stoichiometry, the performance was not much different. This indicated that in the first half of the low-load profile, the stoichiometry λ_a/λ_c = 1.0/1.0 already reached the quality of fuel gas required for the reaction. All of the three load modes exhibited a slow rise in output current as depicted in Figure 8A. In comparison with the optimized performance, the differences between the load modes were minimal, which indicated that the performance in this region was less affected by stoichiometry. Moreover, considering the high-load part of the load modes, the performance oscillated at the highest load, and was incapable of achieving the specified goal. This was because the stoichiometric number λa/λc = 1.0/1.0 was low for high rate reactions. In this situation, there was not enough fuel and humidified water available to

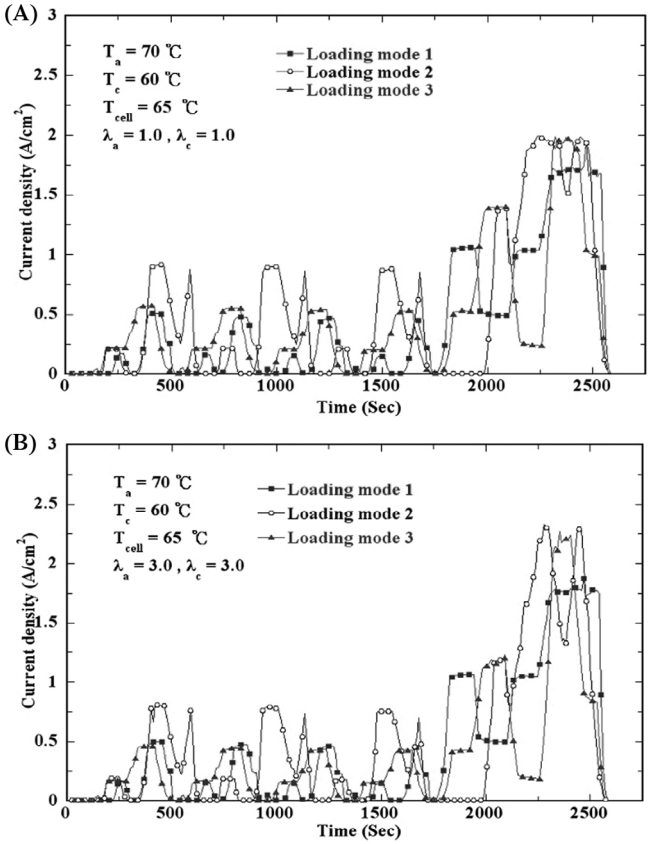

FIGURE 8 Dynamic response of fuel cell subject to various load modes for, A, $\lambda_a = \lambda_c = 1.0$ and, B, $\lambda_a = \lambda_c = 3.0$

improve performance and a decrease in the stoichiometry could render uniform performance.

The average power consumption in load modes 1, 2, and 3 were measured as 0.69, 0.81, and 0.73 W, respectively. Load mode 1 corresponded to the most power decrease, indicating that the load mode has a higher impact on the performance in a low traffic environment. Figure 8B shows the dynamic response of the fuel cell for a high stoichiometric number. As shown in Figure 8B, all of the load modes quickly reached stability without delay in the first half of the test performance, and only load mode 2 gradually decreased. This was because there was a high pressure inside the flow channel at high flow rates and this facilitated the population of the gas by the pressure before a proper diffusion occurred. The gas continued to supply a small amount of fuel during the idle speed of the test process. This would have had the possibility of water accumulation inside the fuel cell. Compared with the optimized performance behavior of the fuel cell, only the load mode 2 presented a noticeable improvement of output performance, indicating that all modes except the second mode were close to the fuel cell-limit. In the high-load test part, after the performance increased and stabilized, some parts showed a shocking phenomenon of performance degradation. Compared to the present performance (below 2.5 A/cm^2), the optimized performance (2.5 A/cm^2) revealed performance reduction. This phenomenon was most evident at the highest load and was because too much gas flow caused the cell to pass too much water, which resulted in flooding and performance reduction. In terms of average power consumption, the average power consumption in load modes of 1, 2, and 3 was 0.70, 0.74, and 0.63 W, respectively. The performance of load mode 3 was the most degraded performance, which indicated that this mode was more affected by high-flow water flooding.

5 | CONCLUSIONS

The focus of this research was to investigate the static and dynamic response of a fuel cell by subjecting it to various load modes. The influence of various parameters such as operating temperature, fuel inlet humidification temperature, stoichiometry, low-temperature environment along with three load modes on the performance of a fuel cell were examined. Three load modes, representing the driving profiles, were adopted to study the dynamic performance of the fuel cell. The voltage of the load modes was dictated to the fuel cell, and the current density of the cell was measured and monitored as the fuel cell response. The optimal fuel cell working temperature, inlet humidification temperature, and stoichiometry have been discussed. The effects of the load modes on the optimized fuel cell parameters and the cold working environment of the cell were investigated experimentally. Based on the experimental results, the main outcomes of the present study can be summarized as follows:

1. In terms of fuel cell working temperature, increasing the cell temperature will lead to an enhancement in the fuel cell performance. The cell temperature directly influenced the moisture inside the cell and the activation of the catalyst layer. However, a very high working temperature elevates the water consumption and causes a dangerous membrane drying. So, choosing a moderate temperature will be advantageous for the performance and the best fuel cell working temperature of the present experiment was 65°C.
2. When the humidification temperature was T_a/T_c = 80°C/70°C, the performance was high but unstable, and the repeatability was low; so the optimized humidification temperature was adopted as T_a/T_c = 70°C/60°C. The fuel inlet humidification temperature was essential as hot gas can carry higher amount of moisture whereas, warm and humid gas improves the wettability of the membrane and affects ion

transport and the membrane-conductivity. However, an excessive humidification temperature may result in water accumulation inside the cell, which may cause flooding and performance degradation.

3. In terms of the impact of stoichiometry, this experiment proved the importance of the appropriate stoichiometry, and the optimal stoichiometric condition was $\lambda_a/\lambda_c = 1.5/2.0$. Although higher stoichiometry can ensure sufficient fuel operating conditions, excessive fuel and upper limit due to catalyst reaction will result in flow channel push.
4. Different test modes can be selected according to the geographical environment or traffic conditions of each place to simulate the energy consumption of a vehicle. Three load modes were adopted to investigate the dynamic performance. In terms of road driving, if the driving mode is relatively flat with low energy requirements, the influence of the parameters is not apparent between the load modes. If the load is high and concentrated, and the driving mode changes rapidly up and down, the fuel cell is easily affected by performance retention.

In the present study, the performance of a single fuel cell was reconnoitered. Although the response behavior of a single fuel cell can provide primary outcomes about the behavior of fuel cells in detail, a stack of fuel cells was required to drive a vehicle in practice. Hence, the study of the dynamic performance of a stack of fuel cells can be subjected to future studies.

ACKNOWLEDGEMENTS

The authors appreciate the financial support from Ministry of Science and Technology, Taiwan under grant number MOST 108-2221-E-027-046-MY2. The authors also appreciate the financially supported by the "Research Center of Energy Conservation for New Generation of Residential, Commercial, and Industrial Sectors" from The Featured Areas Research Center Program within the framework of the Higher Education Sprout Project by the Ministry of Education (MOE) in Taiwan.

ORCID

Mohammad Ghalambaz https://orcid.org/0000-0003-0965-2358

REFERENCES

1. Yousfi-Steiner N, Moçotéguy P, Candusso D, Hissel D. A review on polymer electrolyte membrane fuel cell catalyst degradation and starvation issues: causes, consequences and diagnostic for mitigation. *J Power Sources*. 2009;194(1):130-145.
2. Chen H, Xu S, Pei P, Qu B, Zhang T. Mechanism analysis of starvation in PEMFC based on external characteristics. *Int J Hydrogen Energy*. 2019;44(11):5437-5446.
3. Li J, Lemmon J, Lu Y, et al. Fuel cell with dynamic response capability based on energy storage electrodes. Google Patents, 2019.
4. Arshad A, Ali HM, Habib A, Bashir MA, Jabbal M. Energy and exergy analysis of fuel cells: a review. *Therm Sci Eng Prog*. 2018;9:308-321.
5. Özgür T, Yakaryılmaz AC. A review: exergy analysis of PEM and PEM fuel cell based CHP systems. *Int J Hydrogen Energy*. 2018;43(38):17993-18000.
6. Zhang T, Wang P, Chen H, Pei P. A review of automotive proton exchange membrane fuel cell degradation under start-stop operating condition. *Appl Energy*. 2018;223:249-262.
7. Chen H, Song Z, Zhao X, Zhang T, Pei P, Liang C. A review of durability test protocols of the proton exchange membrane fuel cells for vehicle. *Appl Energy*. 2018;224:289-299.
8. Lee D-J, Wang L. Dynamic and steady-state performance of PEM fuel cells under various loading conditions. Paper presented at: 2007 IEEE Power Engineering Society General Meeting; IEEE; 2007:1-8.
9. Saadi A, Becherif M, Hissel D, Ramadan HS. Dynamic modeling and experimental analysis of PEMFCs: a comparative study. *Int J Hydrogen Energy*. 2017;42(2):1544-1557.
10. Chen T, Liu S, Ruan H. Computer simulation for dynamic characteristics of proton exchange membrane fuel cell. *Int J Mater Struct Integr*. 2016;10(1–3):108-121.
11. Yun S, Cha D, Song KS, et al. Numerical analysis on the dynamic response of a plate-and-frame membrane humidifier for PEMFC vehicles under various operating conditions. *Open Phys*. 2018;16(1):641-650.
12. Yang W, Cha D, Kim Y. Effects of flow direction on dynamic response and stability of nonhumidification PEM fuel cell. *Energy*. 2019;185:386-395.
13. Blal M, Benatiallah A, NeÇaibia A, Lachtar S, Sahouane N, Belasri A. Contribution and investigation to compare models parameters of (PEMFC), comprehensives review of fuel cell models and their degradation. *Energy*. 2019;168:182-199.
14. Hbilate Z, Naimi Y, Takky D. Modelling operation of proton exchange membrane fuel cells-a brief review of current status. *Mater Today Proc*. 2019;13:889-898.
15. Yan Q, Toghiani H, Causey H. Steady state and dynamic performance of proton exchange membrane fuel cells (PEMFCs) under various operating conditions and load changes. *J Power Sources*. 2006;161(1):492-502.
16. Kim S, Shimpalee S, Van Zee J. The effect of stoichiometry on dynamic behavior of a proton exchange membrane fuel cell (PEMFC) during load change. *J Power Sources*. 2004;135(1–2):110-121.
17. Shen Q, Hou M, Yan X, et al. The voltage characteristics of proton exchange membrane fuel cell (PEMFC) under steady and transient states. *J Power Sources*. 2008;179(1):292-296.
18. Santarelli M, Torchio M. Experimental analysis of the effects of the operating variables on the performance of a single PEMFC. *Energ Conver Manage*. 2007;48(1):40-51.
19. Wang X, Wang S, Chen S, Zhu T, Xie X, Mao Z. Dynamic response of proton exchange membrane fuel cell under

mechanical vibration. *Int J Hydrogen Energy*. 2016;41(36):16287-16295.
20. Khan SS, Shareef H, Wahyudie A, Khalid S. Novel dynamic semiempirical proton exchange membrane fuel cell model incorporating component voltages. *Int J Energy Res*. 2018;42(8):2615-2630.
21. Fu K, Tian T, Chen Y, et al. The durability investigation of a 10-cell metal bipolar plate proton exchange membrane fuel cell stack. *Int J Energy Res*. 2019;43(7):2605-2614.
22. Selvaraj AS, Rajagopal TKR. Numerical investigation on the effect of flow field and landing to channel ratio on the performance of PEMFC. *Int J Energy Res*. 2020;44(1):171-191.
23. Jia Y, Sunden B, Xie G. A parametric comparison of temperature uniformity and energy performance of a PEMFC having serpentine wavy channels. *Int J Energy Res*. 2019;43(7):2722-2736.
24. Yin Y, Wang X, Zhang J, Shangguan X, Qin Y. Influence of sloping baffle plates on the mass transport and performance of PEMFC. *Int J Energy Res*. 2019;43(7):2643-2655.
25. Wei G, Lu J, Zhang Q, Zhu F, Yan X, Zhang J. Analyze the effects of flow mode and humidity on PEMFC performance by equivalent membrane conductivity. *Int J Energy Res*. 2019;43(9):4592-4605.
26. Minutillo M, Perna A. Behaviour modelling of a PEMFC operating on diluted hydrogen feed. *Int J Energy Res*. 2008;32(14):1297-1308.
27. Chen H, Zhao X, Qu B, Zhang T, Pei P. Evaluating the gas distribution quality of PEMFC in dynamic response: severe condition of delayed gas supply. *Energy Procedia*. 2019;158:2290-2298.
28. Kim B, Cha D, Kim Y. The effects of air stoichiometry and air excess ratio on the transient response of a PEMFC under load change conditions. *Appl Energy*. 2015;138:143-149.
29. He Y, Chen H, Qu B, Zhang T, Pei P, Liang C. Analysis of proton exchange membrane fuel cell reactant gas dynamic response and distribution quality. *Energy Procedia*. 2018;152:667-672.
30. Barbir F, Braun J, Neutzler J. Effect of collector plate resistance on fuel cell stack performance. *Proton Conduction Membrane Fuel Cells II*. 1999;98(27):400-406.
31. Yoon W, Huang X, Fazzino P, Reifsnider KL, Akkaoui MA. Evaluation of coated metallic bipolar plates for polymer electrolyte membrane fuel cells. *J Power Sources*. 2008;179(1):265-273.
32. Li H, Tang Y, Wang Z, et al. A review of water flooding issues in the proton exchange membrane fuel cell. *J Power Sources*. 2008;178(1):103-117.
33. Ji M, Wei Z. A review of water management in polymer electrolyte membrane fuel cells. *Energies*. 2009;2(4):1057-1106.

How to cite this article: Yang T-F, Sheu B-H, Ghalambaz M, Yan W-M. Effects of operating parameters and load mode on dynamic cell performance of proton exchange membrane fuel cell. *Int J Energy Res*. 2020;1–14. https://doi.org/10.1002/er.5942